

# Novel Methods for Detecting Conductor Breaks in Power Lines

Kanchanrao Dase, James Colwell, and Shreenivas Pai  
*Schweitzer Engineering Laboratories, Inc.*

Presented at the  
50th Annual Western Protective Relay Conference  
Spokane, Washington  
October 10–12, 2023

Originally presented at the  
76th Annual Conference for Protective Relay Engineers, March 2023

# Novel Methods for Detecting Conductor Breaks in Power Lines

Kanchanrao Dase, James Colwell, and Shreenivas Pai, *Schweitzer Engineering Laboratories, Inc.*

**Abstract**—Several single-ended and multi-ended broken conductor detection methods are known to the power system industry. This paper summarizes commonly known broken conductor detection methods and points out their limitations. Two novel single-ended broken conductor detection methods that rely on the series arcing phenomena caused by the conductor break are introduced in this paper. Benefits of the proposed methods over the commonly known detection methods are highlighted. The proposed methods are applicable for transmission and sub-transmission lines and are expected to detect conductor breaks in tapped feeders and distribution systems. This paper presents five broken conductor field events from 110 kV, 138 kV, and 220 kV lines that validate the two novel methods.

## I. INTRODUCTION

Power line conductors gradually weaken as they are exposed to environmental conditions and natural or human-caused mechanical stresses [1]. If not repaired or replaced, these conductors will eventually break and fall to the ground. The subsequent shunt fault and reclosing attempts may cause stress on the power system and shorten the live span of the equipment feeding the fault. Moreover, these faults may ignite wildfires, endangering lives and property. Therefore, detecting broken conductors before they fall to the ground is essential. We discuss the commonly known broken conductor detection methods and their limitations in Section II.

Analyzing the arc initiated by a conductor break can also help detect the broken conductor condition. Once the arc initiates from the conductor breaks, the sustenance of the arc is a function of arc voltage, electric field, arc temperature, and varying levels of ionization of the air [2]–[5]. This paper defines the occurrence of the arc caused by a physical discontinuity in the circuit as series arcing. There are several examples of physical discontinuities in circuits: conductor break, opening of a load interrupting disconnect switch, or opening of circuit breaker pole.

The series arc acts as a medium through which the current continues to flow until the arc extinguishes and interrupts the current. For a broken conductor condition, as the distance between the broken conductor ends increase, the series arc length is expected to increase, increasing the arc resistance [6]–[7]. This series arc can be electrically represented as variable resistance at the broken conductor location in series with the affected phase impedance. Refer to Section III for more explanation on the concept of series arcing.

Power systems with stiff voltages have no significant changes in the terminal voltage on either end of a series fault such as an open-phase condition. For such a power system, the series arc introduces increasing resistance that causes reduction

in the current magnitude of the affected phase. Signs of decrements of the phase current magnitude over a significant time is the basis of the first proposed method for detecting broken conductors. The second proposed method relies on monitoring the estimated phase resistance of the line. This method looks for increasing values of the estimated phase resistance over time. The two proposed novel methods are single-ended and are suitable for transmission, sub-transmission, and distribution systems. These methods are described in detail in Sections IV and V. Benefits of using these methods over other falling conductor protection methods are explained in Section VI.

This paper presents five separate broken conductor field events from 110 kV, 138 kV, and 220 kV lines. Three of these events have recordings from both local and remote terminals. In total, eight field event recordings are used to validate the proposed methods. Performance analysis of these methods is done in Section VII. The conclusions of the paper are covered in Section VIII.

## II. SUMMARY OF BROKEN CONDUCTOR DETECTION METHODS

Broken conductor detection methods can be classified as either single- or multi-ended. This section briefly describes the known broken conductor methods and their limitations.

### A. Single-Ended Methods

Single-ended broken conductor detection methods are based on either unbalanced current, harmonics generated from a downed broken conductor (high-impedance faults [HIFs]), line charging current, or voltage distortion.

#### 1) Unbalanced Current Method

Detection through use of the unbalanced current method requires the unbalance (e.g.,  $|I_2/I_1|$ ) to be higher than a certain threshold (typically 0.2) for a significant time (e.g., 5 to 60 seconds). Using  $|I_2/I_1|$  has limited effectiveness and shortcomings mainly because of elevated  $|I_2/I_1|$  seen at all the network locations upstream of the actual break point. Therefore, detection of broken conductor using  $|I_2/I_1|$  is primarily used as an alarm [8].

#### 2) HIF Method

A broken conductor may become a downed conductor and trigger an HIF. HIFs can be detected by using signatures in the measured signal quantities, mainly the currents. This method uses an adaptive tuning process and gets adapted to the ambient noise profile, increasing the security of the HIF detection element [9]. However, signatures of an HIF in the signal

quantities are not available unless the conductor contacts the ground path. Because not all broken conductors convert into HIFs, the broken conductor condition may remain undetected.

### 3) *Line Charging Current Method*

Detection using the line charging current method requires the measured current to be less than the total line charging current and leading the associated phase voltage by approximately  $90^\circ$  [8]. This method is more suitable for transmission and sub-transmission lines. However, it is not suitable for distribution systems and has a limited zone for protection. This method can also have a delayed detection because the intelligent electronic device (IED) looks for signs of charging current, which is possible only after the series arcing caused by the conductor break extinguishes. Field events have demonstrated that during the series arcing period, the current magnitude of the affected phase decreases, and so the ground or negative-sequence overcurrent protection may operate. In these cases, the IED may issue a trip signal before detecting the broken conductor condition. Refer to Section VI for such an event. The IED, if configured, may issue multiple auto-reclosures on to a permanent fault, causing stress on the power system.

### 4) *Voltage Distortion Method*

Increased voltage distortions and zero-sequence voltage magnitudes have been observed for an open-phase condition in a power line connected to an inverter-based resource (IBR) system. Therefore, overvoltage elements operating on 3V0 or total harmonic distortion (THD) in voltages can be used to detect an open-phase condition [10]. This detection scheme has increased dependability for low loading conditions. However, 3V0 in meshed systems may not change for an open-phase condition (as will be shown later) and the THD methods uses the characteristics of IBRs. Therefore, this method is only suitable for power lines that are directly connected to the IBR system.

## B. *Multi-Ended Methods*

The multi-ended detection of broken conductors can be classified as voltage- and impedance-based methods. The multi-ended algorithms discussed here require time-aligned voltage and/or current data from IEDs stationed at different locations in the power system network. Accessing these data relies upon communications infrastructure that may not be always available.

### 1) *Voltage-Based Methods*

These methods employ synchronized local and remote voltages for detection. The most basic method requires that the downstream voltage be less than a set threshold or a considerable difference in the voltage on each side of a conductor break [11].

Another method declares a broken conductor when the rate-of-change of phase voltages on either side of the break have opposite polarity and exceed a certain threshold. This method requires the use of phasor measurement units (PMUs) [12].

Monitoring the zero- and negative-sequence voltage magnitudes can also be used to detect conductor breaks. As the

broken conductor falls toward the ground, these magnitudes are greater in the PMU farther from the source compared to the ones in the PMU closer to the source. If the magnitudes rise higher than a threshold for a predetermined time, a broken conductor is declared [12].

Lastly, the zero-sequence and negative-sequence angle relationships can also be monitored among the PMUs for a certain angular relation to declare a broken conductor [12].

These voltage-based methods are more suitable for systems that can have changes in voltage for an open-phase condition. These methods may not detect a broken conductor in transmission or meshed distribution systems that have stiff voltages. The analysis of the field events presented in Section VII show no significant change in voltage magnitudes before and after the conductor breaks. These voltage magnitude changes were too small to be relied upon.

### 2) *Impedance-Based Method*

This method uses time-synchronized local and remote current and voltage phasors. First, impedances for each phase of each terminal are calculated. Then a ratio of the change in impedance is calculated by subtracting a previous impedance value from the present value and then dividing the difference by the previous value. If the ratio exceeds a threshold with no assertion of shunt fault detection, a broken conductor condition is declared [13]. Setting a threshold for the ratio of the change in impedance to optimize the dependability and security of this method can be challenging. A higher threshold will restrain the method from asserting for a broken conductor near the center of a power line that has significant charging current. On the other hand, setting a lower threshold can cause a false broken conductor assertion for an external loss-of-load condition.

Recognizing the limitations of the existing broken conductor methods, let us understand the concept of series arcing caused by a conductor break and the two novel single-ended detection methods based on it.

## III. CONCEPT OF SERIES ARCING

When a physical break occurs in a current-carrying conductor, an arc forms at the break point. Once the series arc is initiated in the air, the arc voltage, electric field, arc temperature, and ionization of air all contribute in sustaining the arc [2]–[5]. This paper defines the occurrence of such an arc as series arcing. Circuit breakers, load-interrupting disconnect switches, or conductor breaks may initiate series arcing while interrupting the current. The mechanism of the arc extinction is different for circuit breakers compared to that of load-interrupting disconnect switches or conductor breaks because of the dielectric medium. However, the theory of arc extinctions through a load-interrupting disconnect switch or conductor break are similar. The main difference is the speed at which the ends of the series arc separate. In case of free-falling broken conductor, the linear distance between the ends of the series arc may increase faster than the distance between the contacts of an opening disconnect switch. The following summarizes the concept of series arc extinction in terms of arc voltage as described in [4].

Fig. 1 shows a section of a grid. Here, the power line is in parallel with the mesh network. Consider an occurrence of series arcing caused by a conductor break in the power line. This series arcing is represented as a variable resistance  $R_{ARC}$  in Fig. 1. Typically, the grid loading is not affected by the open-phase conditions occurring in power lines. In Fig. 1, if an open phase occurs in the power line, the respective phase current is redistributed through the mesh network such that there is no change in the incoming current ( $I_S$ ) and the outgoing current ( $I_R$ ) before and after the open-phase condition.

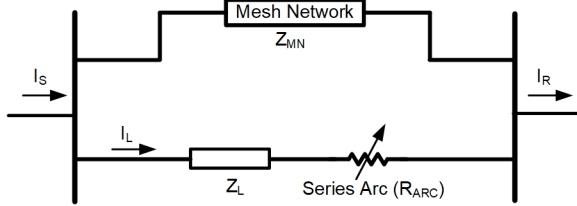


Fig. 1. Representation of a part of a grid with an occurrence of a conductor break in the power line parallel with the mesh network.

When the power line is healthy, the following equation is true.

$$(I_S - I_{L\_BCB}) \cdot Z_{MN} = I_{L\_BCB} \cdot Z_L \quad (1)$$

where:

$I_{L\_BCB}$  is the steady state current through the power line before the conductor break in the line

$Z_{MN}$  is the mesh network equivalent impedance

$Z_L$  is the line impedance

Rearranging the terms in (1),

$$I_S \cdot Z_{MN} = I_{L\_BCB} \cdot (Z_L + Z_{MN}) \quad (2)$$

When the conductor breaks and the series arcing extinguishes, the open-circuit voltage across the ends of the broken conductor segments can be expressed as shown in (3).

$$V_{ARCOC} = I_S \cdot Z_{MN} \quad (3)$$

Equating (2) and (3), we get open-circuit voltage across an extinguished arc, as expressed in (4).

$$V_{ARCOC} = I_{L\_BCB} \cdot (Z_L + Z_{MN}) \quad (4)$$

Equation (4) demonstrates that as the arc voltage drop approaches  $I_{L\_BCB} \cdot (Z_L + Z_{MN})$  value, the arc extinguishes.

The real-time arc voltage drop is equal to  $I_L \cdot R_{ARC}$ . For a conductor break, the series arc resistance is expected to increase with time and the current through it may decrease. Experimental studies have indicated that the voltage drop across the arc takes some time to approach the voltage value calculated in (4) [4]. This time is related to the duration of the series arc. Therefore, the duration of series arcing may vary depending on the magnitude of the current before the conductor break, line impedance, and equivalent impedance of the parallel mesh network. Test data from [4] have shown occurrences of series arcing caused by the opening of a disconnect switch for initial current values as low as 25 A. The same could be true for the occurrences of series arcing through conductor breaks.

Equation (4) is independent of the system voltage, suggesting that series arcing is possible in meshed distribution systems (e.g., ring type distribution system).

Equation (4) is not applicable for conductor breaks in radial feeders, such as the one shown in Fig. 2. For conductor breaks in radial feeder, the series arc is expected to extinguish when the arc voltage drop approaches the system voltage.

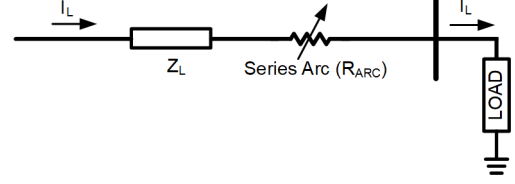
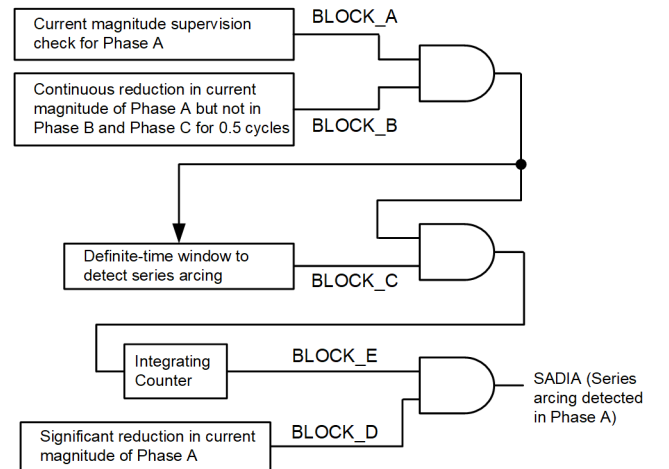


Fig. 2. Representation of a conductor break in radial feeder.

For radial feeders with constant current loads, the current magnitude during the series arc may not decrease. However, the combination of constant power or impedance loads along with constant current loads forces the current to drop as the series arc resistance increases.

#### IV. PROPOSED METHOD FOR DETECTING SERIES ARCING BY MONITORING INCREMENTAL REDUCTIONS IN THE PHASE CURRENT MAGNITUDE

Fig. 3 presents an overview of the series arcing detection through the current-reduction logic. This algorithm mainly looks for signs of incremental reduction in the current magnitude only in one of the phase currents for a stipulated time (e.g., three power system cycles). When the respective phase current magnitude experiences significant reduction as compared to the earlier balanced system current magnitude, the logic declares detection of series arcing. This section describes the series arcing detection through current-reduction logic in detail and outlines the thresholds used for validating the field events presented in the paper.



Note: Logic is for Phase A. Logic for Phase B and Phase C is similar.

Fig. 3. Overview of series arcing detection logic by monitoring reductions in the phase current magnitude.

Fig. 4 shows the logic bits of the series arcing detection method by monitoring reductions in the phase current

magnitude for a Phase C broken conductor field event. Fig. 4 can be used as a reference to better understand the logic flow.

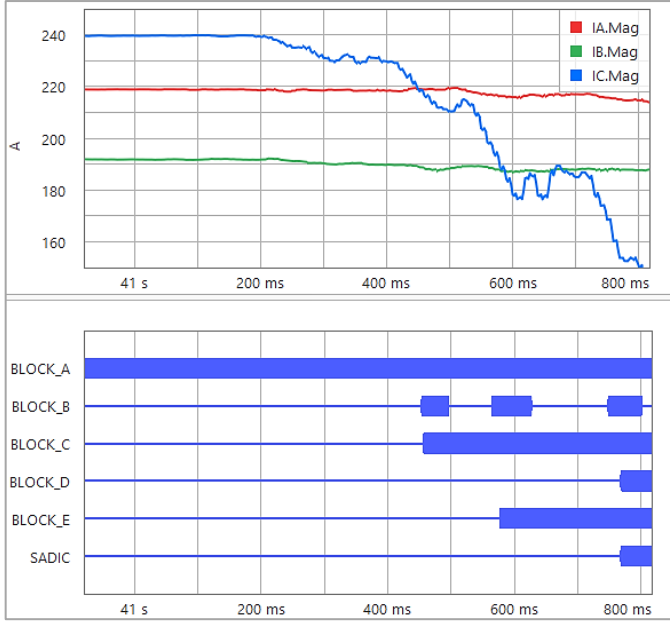


Fig. 4. Logic bits of the series arcing detection method by monitoring the reductions in the phase current magnitude for a Phase C broken conductor field event.

#### A. Current Magnitude Supervision Check

Series arcing is more likely to occur when a conductor break or the opening of a disconnect switch interrupts the load current. Set a minimum threshold for the phase current magnitude to filter out low loading cases. The BLOCK\_A of the series arcing detection algorithm requires the current to be greater than a minimum threshold that depends on the IED sensitivity. In Fig. 4, the Phase C current magnitude remained high enough to keep the BLOCK\_A bit asserted.

#### B. Incremental Reductions in the Phase Current Magnitude

This logic looks for reductions in the current magnitude of one phase with no decrement in the current magnitudes of the other two phases. When this condition, along with the minimum current supervision check (BLOCK\_A), is satisfied for a predetermined time, e.g., 0.5 power system cycle, a definite-time window opens for detecting possible series arcing. Defining the threshold to compare the incremental reductions in the phase current magnitude can be challenging to maintain dependability of the algorithm and avoid false assertions. In this paper, we chose the minimum threshold to check the magnitude reduction based on the field events data. Note that a sudden reduction in the phase current magnitude is not expected during the series arcing caused by the conductor break. Therefore, we also set a higher limit in the incremental drop of the phase current magnitude. This can filter out cases where the current magnitudes quickly drop to zero when the circuit breaker trips the line.

#### C. Definite-Time Window to Detect Series Arcing

The definite-time window detecting possible series arcing is open only for the phase that has decreasing current magnitude.

The defined time for this window can encompass the duration of the series arcing, so the algorithm has enough time to detect series arcing phenomena. The broken conductor field events described in this paper exhibit series arcing durations ranging from 0.2 to 0.7 seconds. Considering this range, we select a definite-time window of 18 power system cycles. The definite-time window is closed upon initiation of a shunt fault or when the respective phase current magnitude falls lower than a minimum threshold (deassertion of BLOCK\_A).

#### D. Significant Reduction in the Phase Current Magnitude

This logic, defined as BLOCK\_D in Fig. 3, asserts when there has been a significant drop in the phase current magnitude within the definite time window. For the field event analysis, a reduction of 25 percent was considered.

#### E. Integrating Counter

The integrating counter calculates the processing counts during which BLOCK\_A and BLOCK\_B are asserted while the definite-time window is open (BLOCK\_C is asserted). The integrating counter helps to differentiate an open-phase condition caused by the opening of a breaker pole or through the extinction of series arcing caused by a conductor break. When a breaker pole opens, the corresponding phase current reduces quickly and drops to zero in less than the breaker pole-open time (two to three power system cycles), whereas the occurrence of series arcing for a conductor break causes gradual reduction in the affected phase current magnitude, as shown in Fig. 4 for a Phase C broken conductor event. Note that BLOCK\_A and BLOCK\_B may not be continuously asserted as shown in Fig. 4. Implementing an integrating counter instead of a normal pickup delay timer ensures the time delay in detecting series arcing condition is minimized. For the integrator counter, each count equals the duration of 1/8th of a power system cycle. When the integrator count exceeds a threshold, the output of the integrating counter asserts. As explained earlier, the count threshold should be slightly more than the number of counts required for the breaker pole to open.

Finally, the logic declares detection of series arcing when the output of the integrating timer and the BLOCK\_D logic have asserted. Note that the detection of series arcing by monitoring the current reductions is not suitable for radial feeders with constant current loads.

## V. PROPOSED METHOD FOR DETECTING SERIES ARCING BY ESTIMATING THE PHASE RESISTANCE VALUES

Typically, transmission, sub-transmission, and, some distribution systems consist of mesh networks. For any series faults, e.g., open-phase, in these networks, the respective phase current of the affected line is redistributed in the network, resulting in no loss of load. The redistribution of the currents for such a series fault keeps the system voltage stiff. Fig. 5 represents such a power system. In Fig. 5, if an open phase occurs in Phase A of the line, the Phase A current is redistributed through the mesh network, and there is no change in the currents coming into Terminal S ( $I_S$ ) and going out of Terminal R ( $I_R$ ). This also results in stiff voltages at the Terminals S and R for any open-phase condition on the power

line. With this consideration, the following describes an approach to detect series arcing by estimating the phase resistances.

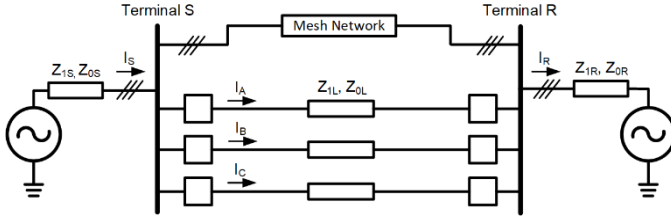


Fig. 5. Representation of a power line in a mesh power system network.

Equation (5) gives the estimated Phase A resistance of a transposed power line by using the voltage drop equation [14]. For simplicity, assume no additional zero-sequence mutual couplings are linking the power line.

$$R_{A\_EST} = \text{Real} \left( \frac{V_{AS} - V_{AR} - (I_B + I_C) \cdot Z_M}{I_A} \right) \quad (5)$$

where:

$V_{AS}$  is the local terminal Phase A voltage

$V_{AR}$  is the remote terminal Phase A voltage

$Z_M$  is the phase-to-phase mutual impedance

Fig. 6 shows a series arcing caused by the conductor break in Phase A of the power line. This series arcing is represented as a variable resistance ( $R_{ARC}$ ). As the series arcing progresses in time,  $R_{ARC}$  is expected to increase, because the length of the arc grows as the distance between the broken conductor ends increase. During the arcing period, the estimated phase resistance ( $R_{A\_EST}$ ) of the power line calculated by using (5) should equal to the sum of the actual resistance of Phase A ( $R_A$ ) and the variable arc resistance ( $R_{ARC}$ ). Under normal loading conditions (without any series arc), the estimated Phase A resistance ( $R_{A\_EST}$ ) calculated by (5) should equal to the actual resistance of Phase A ( $R_A$ ). Therefore, by monitoring the increase in the Phase A resistance by using (5), the occurrence of series arcing and thus a broken conductor can be detected. Note, (5) uses synchronized local and remote measurements to detect series arcing, making the use of (5) a multi-ended approach. Next, we describe the extension of this approach to detect series arcing without using the remote voltages.

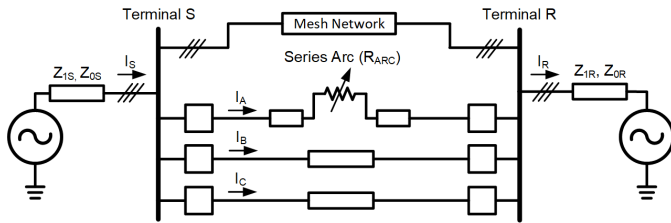


Fig. 6. Representation of series arcing caused by the broken conductor in Phase A of the power line.

The proposed method assumes the occurrence of series arcing in only one phase while the other two phases remain healthy. Given this assumption and because the arc resistance varies by length, the corresponding estimated phase resistance should increase during series arcing for a significant amount of

time (e.g., three power system cycles) compared to the other two phases. Now, consider series arcing in Phase A, while Phase B and Phase C are assumed to be healthy. With this assumption, the remote terminal voltages of Phase B and C, calculated using only the local analogs and line parameters, are estimated correctly by using (6) and (7), respectively.

$$V_{BR\_EST} = V_{BS} - I_{LOOPB} \cdot Z_{1L} \quad (6)$$

$$V_{CR\_EST} = V_{CS} - I_{LOOPC} \cdot Z_{1L} \quad (7)$$

where:

$V_{BS}$  and  $V_{CS}$  are the local terminal Phase B and Phase C voltages

$I_{LOOPB} = I_B + k_0 \cdot I_G$  and  $I_{LOOPC} = I_C + k_0 \cdot I_G$  are the Phase B and Phase C loop currents

$k_0 = \frac{Z_{0L} - Z_{1L}}{3 \cdot Z_{1L}}$  is the zero-sequence compensation factor

$Z_{1L}$  is the positive-sequence line impedance

$Z_{0L}$  is the zero-sequence line impedance

Using (6) and (7), calculate the remote terminal Phase A voltage as expressed in (8).

$$V_{AR\_EST} = V_{GR\_EST} - (V_{BR\_EST} + V_{CR\_EST}) \quad (8)$$

where:

$V_{GR\_EST}$  is the remote terminal ground voltage

Typically, power systems networks have stiff and balanced voltages, making the ground voltage too small to consider. However, if there is significant ground voltage before an open phase occurs, it cannot be ignored. For such cases, calculate  $V_{GR\_EST}$  by using (9).

$$V_{GR\_EST} = V_{GL} - I_G \cdot Z_{0L} \quad (9)$$

where:

$V_{GL}$  is the local terminal ground voltage

$I_G$  is the ground current through the affected power line

When the changing series arcing resistance ( $R_{ARC}$ ) is introduced in one phase of the line, additional ( $R_{ARC}/3$ ), in parallel with the positive- and negative-sequence network, is also introduced in the zero-sequence impedance of the line [15]. Therefore, using (9) to estimate  $V_{GR\_EST}$  will be erroneous from the instance of physical break in the conductor. However,  $V_{GR\_EST}$  can be approximated by latching to its value from a time just before the conductor break. Therefore, (8) can be rewritten as:

$$V_{AR\_EST}' = V_{GR\_EST}|_{BCB} - (V_{BR\_EST} + V_{CR\_EST}) \quad (10)$$

where:

$V_{GR\_EST}|_{BCB}$  is the latched value from a time just before the conductor break (BCB)

The assumption of latching  $V_{GR\_EST}$  is true for power systems that have stiff voltages for an open-phase event in the power line. Accurate estimation of the series arc resistance requires accurate  $V_{GR\_EST}$ . However, the proposed detection method looks at the trend, especially the variation of the

estimated phase resistance rather than for its accuracy. Considering this and using  $V_{AR\_EST'}$  from (10) in place of  $V_{AR}$  in (5), we get another estimated resistance of Phase A as expressed in (11). Equation (11) contains only the local analogs and line parameters, making it a single-ended approach in estimating the phase resistance.

$$R_{A\_EST'} = \text{Real} \left( \frac{V_{AS} - V_{AR\_EST'} - (I_B + I_C) \cdot Z_M}{I_A} \right) \quad (11)$$

Similar to (11), use local voltages and currents and line parameters to estimate the resistance of Phase B and Phase C, as expressed in (12) and (13), respectively.

$$R_{B\_EST'} = \text{Real} \left( \frac{V_{BS} - V_{BR\_EST'} - (I_A + I_C) \cdot Z_M}{I_B} \right) \quad (12)$$

$$R_{C\_EST'} = \text{Real} \left( \frac{V_{CS} - V_{CR\_EST'} - (I_A + I_B) \cdot Z_M}{I_C} \right) \quad (13)$$

Analysis of the field events presented in this paper have shown no significant difference in the estimated arc resistance with or without the use of the remote ground voltage,  $V_{GR\_EST}|_{BCB}$ . This could mainly be due to the stiff system voltages even during the arcing period, supporting the assumption made for the derivation of (11), (12), and (13). Subtracting the actual phase resistance from the estimated phase resistance gives the corresponding estimated arc resistance during the occurrence of series arcing, as expressed in (14), (15), and (16). The estimated arc resistance values can be erroneous in the case of missing mutual coupling voltage drops from the parallel lines. However, this is not an issue for the proposed series arcing detection method because the method relies on the rate of change trend of the estimated arc resistance values rather than its accuracy.

$$EARC\_RA = R_{A\_EST'} - R_{A\_SELF} \quad (14)$$

$$EARC\_RB = R_{B\_EST'} - R_{B\_SELF} \quad (15)$$

$$EARC\_RC = R_{C\_EST'} - R_{C\_SELF} \quad (16)$$

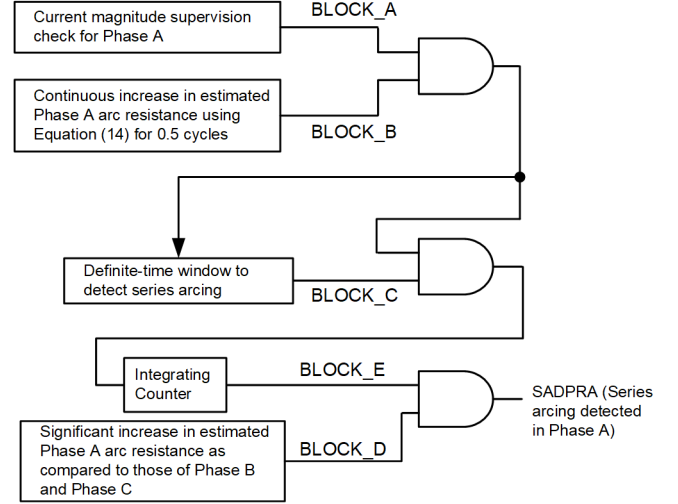
where:

$R_{A\_SELF}$ ,  $R_{B\_SELF}$ , and  $R_{C\_SELF}$  are the Phase A, Phase B, and Phase C self resistances, respectively

Under normal conditions, Equations (14), (15), and (16) are true and the estimated arc resistance values for each phase should be zero. However, for an occurrence of series arcing in one phase, the equation for the estimated arc resistance is only true for the affected phase. The estimated arc resistances for the remaining two phases are wrong because of the missing arc voltage drop in their equations. This is not a concern because the phases with incorrectly estimated arc resistance values can be easily eliminated. The estimated arc resistance value for the phase with series arcing should be positive and increase with time. So, any phase that has negative or steady values of estimated arc resistance is definitely not the phase with series arcing. Alternatively, the phase current magnitudes can also be monitored while estimating the arc resistance values for each

phase. The phase that has increasing values of estimated arc resistance and decreasing current magnitude is the one with series arcing.

Fig. 7 gives an overview of the series arcing detection logic by estimating the phase resistance values. The flow of the algorithm is similar to that of the current reduction logic described in Section IV. Note the detection of series arcing by estimating the phase resistance values is not suitable for radial feeders with constant current loads.



Note: Logic is for Phase A. Logic for Phase B and Phase C is similar.

Fig. 7. Overview of series arcing detection logic by estimating the phase resistance values.

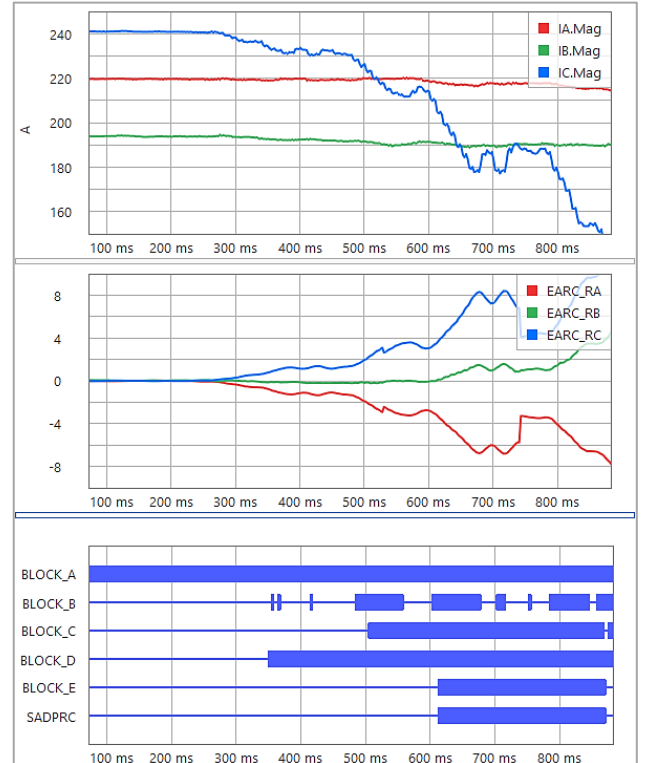


Fig. 8. Logic bits of the series arcing detection method by estimating the phase resistance values for a Phase C broken conductor field event.

Fig. 8 shows the logic bits of the series arcing detection method by estimating the phase resistance values for a Phase C

broken conductor field event. Fig. 8 can be used as a reference to better understand the logic flow. EARC\_RA, EARC\_RB, and EARC\_RC are the estimated series arc resistances for Phases A, B, and C in secondary ohms, respectively.

## VI. BENEFITS OF USING THE PROPOSED SERIES ARCING DETECTION METHODS

### A. Fast Detection of Broken Conductor

Broken conductors can take more than one second from the instant of the conductor break to hit the ground [12]. Taking this into account, IEDs processing logics in the order of milliseconds can have adequate time to declare such a condition. However, taking significant time may not be always helpful. The broken conductor field event in Fig. 9 demonstrates why the fast detection of a broken conductor is beneficial.

Fig. 9 shows the phase currents of the 110 kV transmission line during the time frame of the Phase C conductor break. Corresponding protection and the two proposed series arcing detection bits are also included. After the conductor break, the series arcing causes reduction in the respective phase current magnitude. This results in the assertion of the unbalanced (ground) overcurrent element and the IED issues a trip command based on a communication-assisted protection scheme. After the initial trip, the relay auto-recloses and trips again on switch-on-to-fault (SOTF) protection. This part of the event is not shown in Fig. 9. In this field event, the detection of the broken conductor before the initial tripping could have blocked the auto-reclose, preventing the shunt fault.

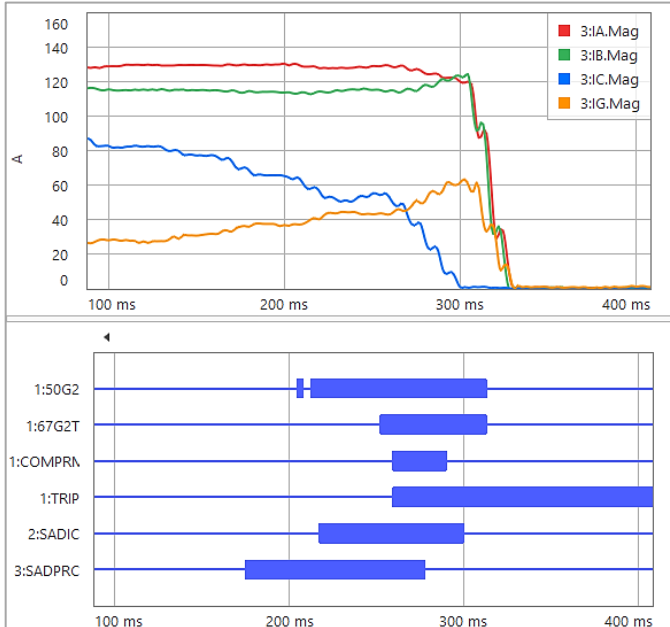


Fig. 9. Phase currents of the 110 kV transmission line during the time frame of the Phase C conductor break.

Using the series arc detection methods in this case may have detected the broken conductor long before the relay tripped on the ground overcurrent element. Playback of this event has shown successful detection of series arcing through the use of the two proposed algorithms. The 1:SADIC and 1:SADPRC

bits in Fig. 9 indicate the detection of the broken conductor in Phase C through current reduction and phase resistance monitoring methods, respectively. Because these detection bits asserted before the IED issued the trip and the current analogs went to zero, they could have been used to block the auto-reclose, preventing the shunt fault.

Note the charging current method of detecting a broken conductor [8] could not have detected this condition. This is because the relay could not measure the charging current before the breakers tripped. When the relay issued the trip command, the series arcing carrying the load current superimposed the charging current.

### B. Security for Loss-of-Load Conditions

Typically, a loss of load is measured by the IED as a steep change in the respective phase current magnitude. The two proposed series arcing detection logics look for signs of gradually decreasing current magnitude or gradually increasing phase resistance for a significant time (e.g., three power system cycles). These conditions restrain the two proposed algorithms from detecting a loss-of-load condition and thus enhance the security of broken conductor detection. Fig. 10 demonstrates an example of 75 percent loss of load in Phase A. For this simulation, the two proposed series arcing detection logics were not asserted and rightly did not declare a broken conductor event.

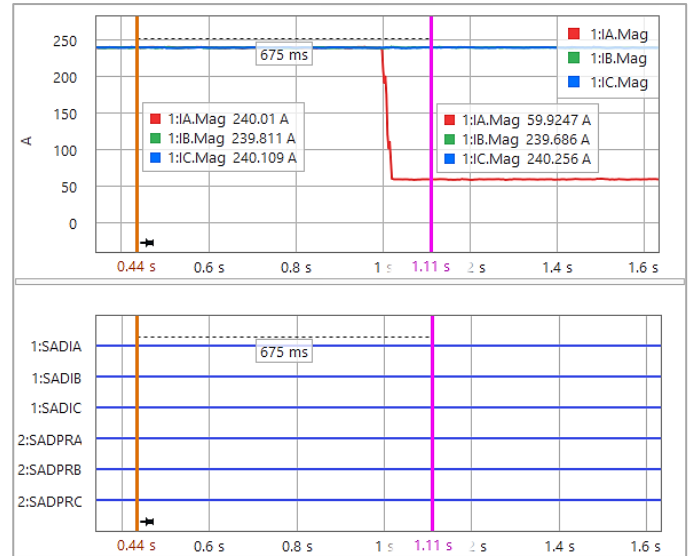


Fig. 10. Simulation of 75 percent loss of load in Phase A.

### C. Capable of Detecting Series Arcing Caused by Broken Conductors Beyond the Protected Line

The two proposed concepts described in the paper are also capable of detecting series arcing occurring beyond the protected line. This means the IEDs of the power lines, having the proposed algorithms, can detect series arcing occurring in any of the taps connected to the power line. This is because the power line feeding current to the tapped feeder can have the signs of decreasing current magnitudes and increasing values of estimated phase resistance in the affected phase. This condition is as if the series arcing is occurring in the protected line. The only difference is that the current magnitude measured by the

IED at the source end will not reduce to a charging current value because the open-phase condition exists in the tapped feeder rather than in the power line.

When we consider the previous example of detecting series arcing in the tapped feeders, the application of detecting series arcing through the use of the two proposed methods can also be extended to the distribution systems. However, the proposed detection methods are not suitable for radial feeders with constant current loads.

In some utilities, sub-transmission or distribution lines are equipped with disconnect switches to interrupt load currents. These disconnect switches produce series arcing while interrupting the load current. The two proposed algorithms may detect these kinds of series arcing, but in all three phases. The series arcing may initiate at different times in the three phases; therefore, adding a delay in the detection methods can help distinguish a single-phase broken conductor event from a three-phase opening of a load interrupter. For noisy loads, the thresholds in the proposed detection methods can be changed to bias towards security. However, because the proposed solutions to detect broken conductor are new, they are meant for analysis and as critical alarms. They may also be used to block auto-reclosures upon series arcing detection followed by an assertion of a trip signal.

#### D. Single-Ended Method

The two proposed algorithms to detect series arcing caused by a conductor break are single-ended methods. Not requiring any synchronized analog data from the remote IEDs make these logics less complex and easy to implement.

### VII. FIELD EVENT ANALYSIS

To validate the proposed series arcing detection methods, we programmed equations into the free-form logic of a protective relay. In total, eight event recordings were used to test the two proposed methods. These eight events recordings were from five separate broken conductor field events that occurred on 110 kV, 138 kV, and 220 kV lines. For three of these events, both local and remote recordings were available. Key readings from the tests are summarized in Table I. Fig. 11–Fig. 18 demonstrate successful detection of broken conductors upon playback of the field events using the proposed current magnitude reduction and estimated phase resistance monitoring methods.

The  $T_{SADI}$  and  $T_{SADPR}$  columns in Table I imply both the proposed series arcing detection methods successfully identified the occurrence of series arcing, hence the detection of broken conductor for each of the field events. Series arcing detection through the current magnitude reduction method took on average about 75 percent of the total series arc duration for

detection. The initiation of series arcing from the field event recordings is taken as an instance where the affected phase current magnitude starts to deviate from its previous value. The total series arcing duration estimated from the field events ( $T_{SAI}$  column in Table I) was in the range of 0.2 to 0.7 seconds. The current magnitude reduction method takes considerable time for series arcing detection mainly because the affected phase current magnitude does not decrease continuously. Collapsing of series arcs into shorter arc lengths increases the current flow momentarily but the increasing distance between the ends of the broken conductor increases the arc resistance, eventually decreasing the current magnitude. Momentary rises between durations of decreasing current magnitudes causes a delay in the detection of a series arc.

The second proposed method of detecting series arcing through the monitoring of phase resistance values uses voltages and currents, making this method more sensitive and faster. From the test results in Table I, the second detection method ( $T_{SADPR}$  column in Table I) took on average around 50 percent of the total series arc duration for detection, 25 percent faster than the first detection method ( $T_{SADI}$  column in Table I).

As noted in Section II, some of the falling conductor detection methods use the signatures of the change in phase, zero-, and negative-sequence voltage. The  $\Delta V_{PH}$ ,  $\Delta V_0$ , and  $\Delta V_2$  columns in Table I show the respective changes in the phase, zero-, and negative-sequence voltages before and after the series arcing. The change in the voltage values are too small and that makes setting thresholds for these voltage changes a challenging task. Ignoring the smaller values, the change in phase voltage were found to be of opposing polarity at either end of the conductor break. This satisfies one of the conditions in one of the methods of detecting falling conductors mentioned in [11] and [12]. However, the change in zero-sequence voltage, which is expected to rise for a broken conductor event, has shown almost no change in most of the events. Therefore, methods that rely on changes in voltage magnitudes may be challenged to detect falling conductors in transmission or meshed distribution systems that have insignificant voltage change for an open-phase condition.

The last column ( $|Z_{SAE}/Z_{SAI}|$ ) in Table I gives the increase in the phase impedance after the extinction of the series arc with reference to corresponding phase impedance before the series arc initiation. The phase impedance is calculated as  $|V_{PH}/I_{PH}|$ . The  $|Z_{SAE}/Z_{SAI}|$  column can be used to validate methods that use the change in impedance to detect broken conductors. The values of the phase impedances after the extinction of series arc are not infinite because the measured current is not zero, but, in fact, is the line charging current between the relay and the conductor break location.

TABLE I  
SUMMARY OF THE TEST RESULTS FROM THE PLAYBACK OF FIELD EVENTS

Event	Terminal	Voltage Level (kV)	$ I_{SAI} $ (A)	$ I_{SAE} $ (A)	$T_{SA}$ (s)	$T_{SADI}$ (s)	$T_{SADPR}$ (s)	$\Delta V_{PH}$ (pu)	$\Delta V_0$ (pu)	$\Delta V_2$ (pu)	$ Z_{SAE}/Z_{SAI} $
1	Local	220	408	67.5	0.21	0.15	0.09	-0.005	0.002	0.008	6
	Remote		420	3.1		0.15	0.10	0.001	-0.001	0.003	135
2	Local	138	287 <sup>a</sup>	1.9 <sup>a</sup>	0.36 <sup>a</sup>	0.23 <sup>a</sup>	0.21 <sup>a</sup>	-0.018 <sup>a</sup>	0.007 <sup>a</sup>	0.014 <sup>a</sup>	151 <sup>a</sup>
	Remote		265 <sup>a</sup>	1.9 <sup>a</sup>		0.20 <sup>a</sup>	0.19 <sup>a</sup>	0.006 <sup>a</sup>	0.007 <sup>a</sup>	0.008 <sup>a</sup>	139 <sup>a</sup>
3	Local	110	127	5.5	0.41	0.27	0.22	-0.032	0.026	0.019	23
	Remote		127	5.5		0.29	0.33	0.011	-0.001	0.010	23
4	NA	220	244	26.5	0.53	0.40	0.25	0.003	0.001	0.001	9
5	NA	138	242	17.2	0.71	0.57	0.35	-0.019	0.004	0.016	14

$|I_{SAI}|$  is current magnitude of the broken conductor phase at an instance of series arc initiation in primary amperes.

$|I_{SAE}|$  is current magnitude of the broken conductor phase at an instance of series arc extinction in primary amperes.

$T_{SA}$  is the estimated duration of series arcing in seconds.

$T_{SADI}$  is the approximate time taken to detect series arcing from the initiation of the arc through the current magnitude reduction method in seconds.

$T_{SADPR}$  is the approximate time taken to detect series arcing from the initiation of the arc through the phase resistance monitoring method in seconds.

$\Delta V_{PH}$  is the change in the broken conductor phase voltage magnitude from an instance of series arc extinction to an instance of series arc initiation in pu.

$\Delta V_0$  is the change in the zero-sequence voltage magnitude from an instance of series arc extinction to an instance of series arc initiation in pu.

$\Delta V_2$  is the change in the negative-sequence voltage magnitude from an instance of series arc extinction to an instance of series arc initiation in pu.

$|Z_{SAE}|$  is the ratio of the magnitude of phase voltage to phase current of the broken conductor phase at the instance of series arc extinction in primary kV.

$|Z_{SAI}|$  is the ratio of the magnitude of phase voltage to phase current of the broken conductor phase at the instance of series arc initiation in primary kV.

<sup>a</sup> These are the estimated values obtained by reconstructing some of the pre-fault data in the event recordings.

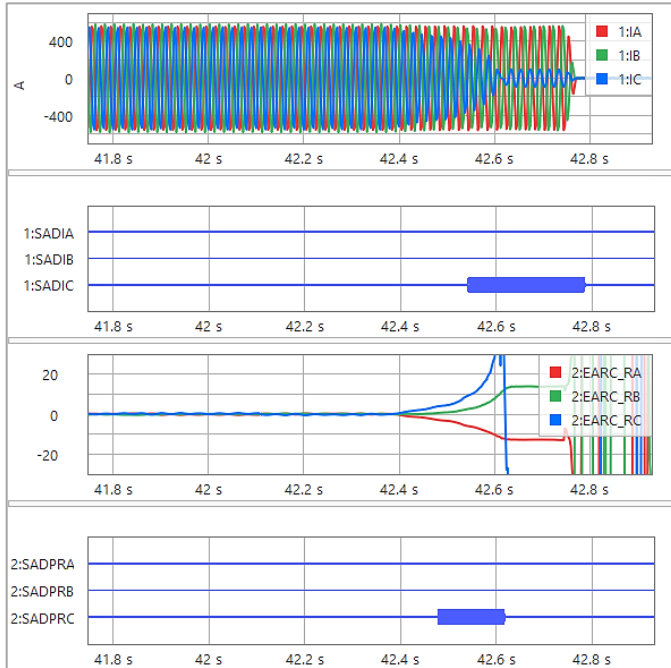


Fig. 11. Series arcing detection bits of the current magnitude reduction method (top) and estimated phase resistance monitoring method (bottom) for Event 1 (local terminal) in Table I.

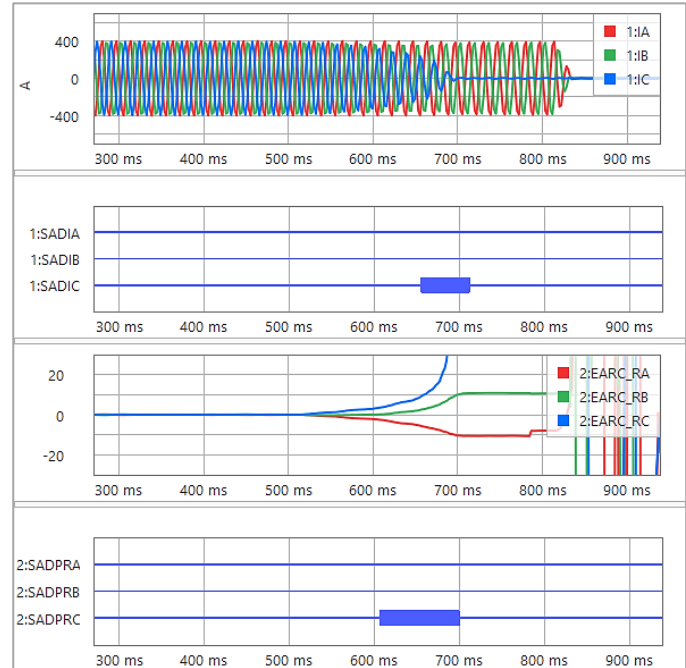


Fig. 12. Series arcing detection bits of the current magnitude reduction method (top) and estimated phase resistance monitoring method (bottom) for Event 1 (remote terminal) in Table I.

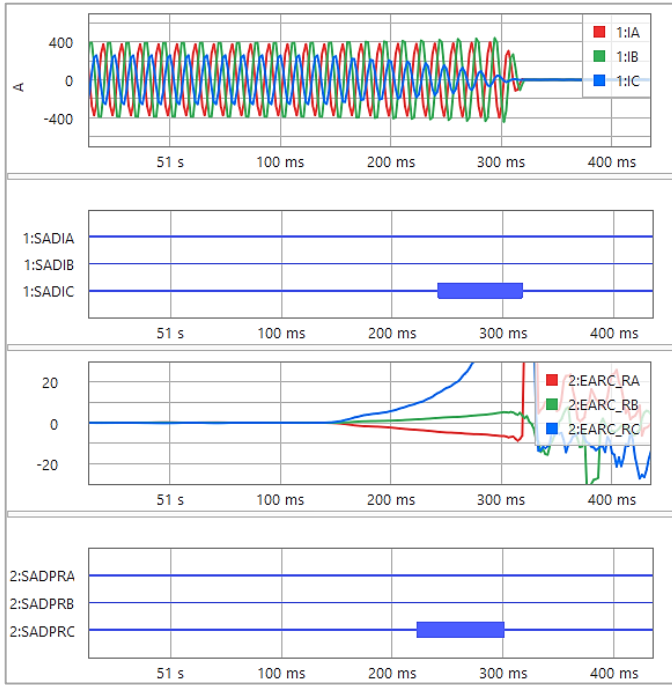


Fig. 13. Series arcing detection bits of the current magnitude reduction method (top) and estimated phase resistance monitoring method (bottom) for Event 2 (local terminal) in Table I.

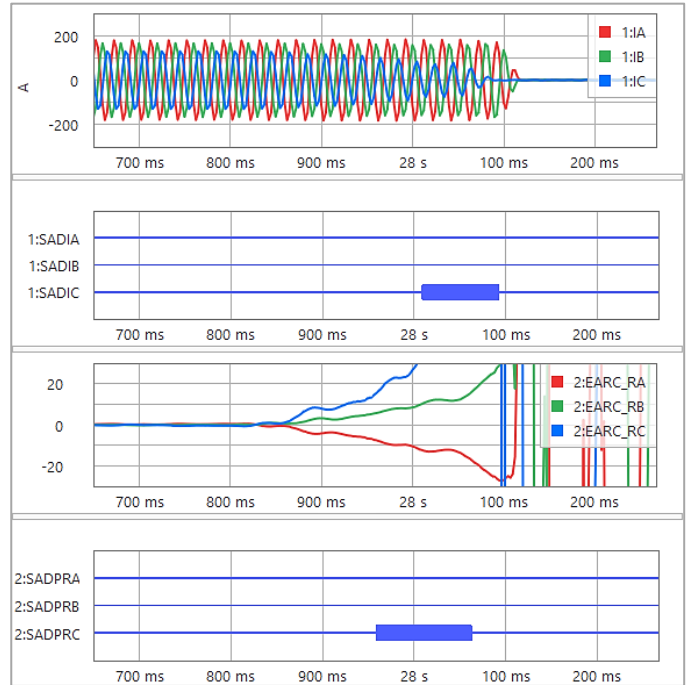


Fig. 15. Series arcing detection bits of the current magnitude reduction method (top) and estimated phase resistance monitoring method (bottom) for Event 3 (local terminal) in Table I.

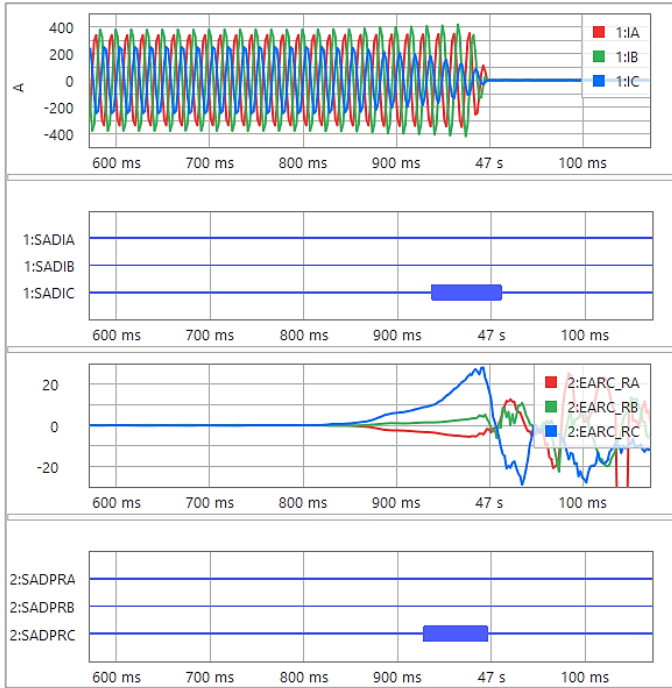


Fig. 14. Series arcing detection bits of the current magnitude reduction method (top) and estimated phase resistance monitoring method (bottom) for Event 2 (remote terminal) in Table I.

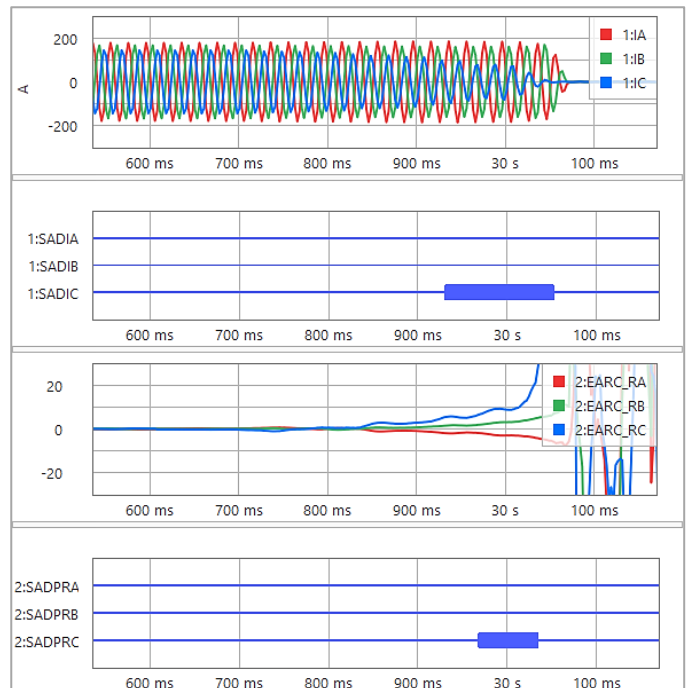


Fig. 16. Series arcing detection bits of the current magnitude reduction method (top) and estimated phase resistance monitoring method (bottom) for Event 3 (remote terminal) in Table I.

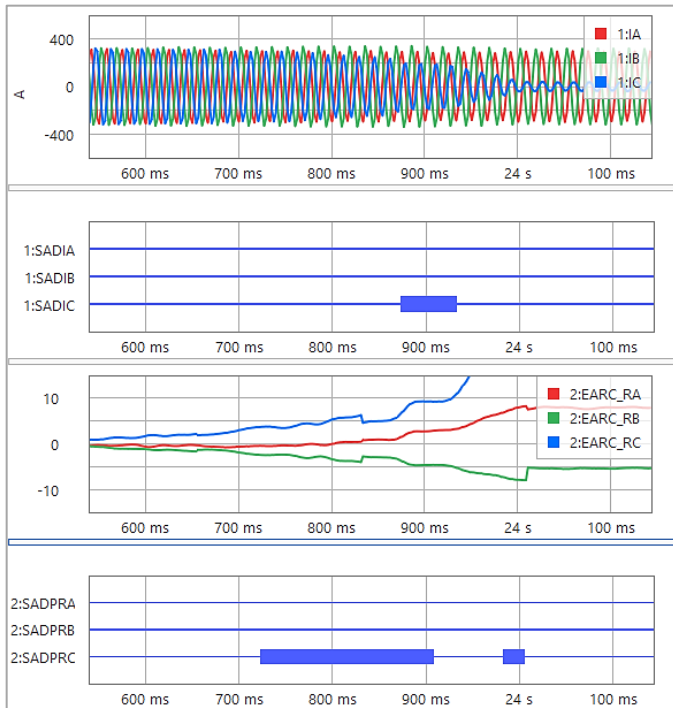


Fig. 17. Series arcing detection bits of the current magnitude reduction method (top) and estimated phase resistance monitoring method (bottom) for Event 4 in Table I.

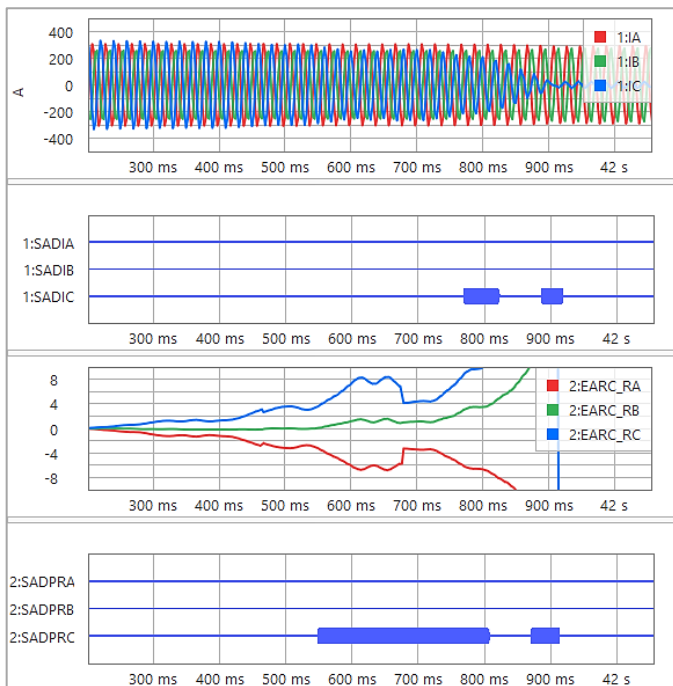


Fig. 18. Series arcing detection bits of the current magnitude reduction method (top) and estimated phase resistance monitoring method (bottom) for Event 5 in Table I.

## VIII. CONCLUSION

This paper revisits the arcing phenomena that occur during the opening of a load-interrupting disconnect switch. Field events presented in this paper have shown similar arcing occurs when a conductor breaks. This paper presents two novel methods to detect series arcing caused by a conductor break.

The first method looks for reduction in the current magnitude over a predetermined time. The second method looks for a substantial increase in the estimated phase resistance over a predetermined time. Detection of broken conductors by using these proposed methods were successful when tested with the eight field event recordings. However, because the proposed solutions to detect broken conductor are new, they are meant for analysis and as critical alarms. They may also be used to block auto-reclose upon series arcing detection followed by an assertion of trip signal.

Fast detection of a broken conductor becomes crucial when attempting to block auto-reclose for lines with sensitive ground or negative-sequence protection. Results from the field events show early detection of series arcing by using the proposed methods can address this issue. The proposed detection methods work for transmission and sub-transmission systems and are expected to work for tapped feeders and distribution systems; however no supporting field events were available at the time of this publication. Of course, these methods are only useful for distribution lines that have circuit breakers. Analysis of the field events has shown detection through use of the current magnitude reduction method requires slightly longer time to detect a broken conductor as compared to the phase resistance monitoring method, which uses currents and voltages.

Existing methods that look for a considerable change in voltage at opposite ends of the line during an open-phase condition are suitable for distribution or weaker power system networks. Field events presented in this paper have shown no significant change in voltage magnitudes before and after the conductor break. Methods that rely on change in impedance before and after the conductor break may have less dependability for a broken conductor near the center of a power line that has significant charging current.

## IX. REFERENCES

- [1] Transpower New Zealand Limited, "TL Conductors and Insulators Fleet Strategy," Document TP.FL 01.00, October 2013. Available: <https://www.transpower.co.nz>.
- [2] J. Slepian, "Extinction of an A-C. Arc," in *Transactions of the American Institute of Electrical Engineers*, Vol. 47, No. 4, pp. 1398–1407, October 1928.
- [3] J. Slepian and A. P. Strom, "Arcs in Low-Voltage A-C. Networks," in *Transactions of the American Institute of Electrical Engineers*, Vol. 50, No. 3, pp. 847–852, September 1931.
- [4] D. F. Peel (2004). Current interruption using high voltage air-break disconnectors. [Phd Thesis 2 (Research NOT TU/e / Graduation TU/e), Electrical Engineering, Technische Universiteit Eindhoven].
- [5] D. Shin (2018). A study of re-ignition phenomena and arc modelling to evaluate switching performance of low-voltage switching devices. [Doctoral Thesis, University of Southampton, 226 pp].
- [6] A.R. Van and C. Warrington, "Reactance relays negligibly affected by arc impedance," *Electrical World*, pp. 502–505, September 19, 1931.
- [7] V. V. Terzija and H.-J. Koglin, "On the modeling of long arc in still air and arc resistance calculation," in *IEEE Transactions on Power Delivery*, Vol. 19, No. 3, pp. 1012–1017, July 2004.
- [8] K. Dase, S. Harmukh, and A. Chatterjee, "Detecting and Locating Broken Conductor Faults on High-Voltage Lines to Prevent Autoreclosing Onto Permanent Faults," 46th Annual Western Protective Relay Conference, Spokane, Washington, October 21–24, 2019.

- [9] D. Hou, "Detection of High-Impedance Faults in Power Distribution Systems," Proceedings of the 33rd Annual Western Protective Relay Conference, Spokane, WA, October 2006.
- [10] J. Gahan, A. Valdez, B. Cockerham, R. Chowdhury, and J. Town, "Field Experience With Open-Phase Testing at Sites With Inverter-Based Resources," Proceedings of the 74th Annual Conference for Protective Relay Engineers, March 2021.
- [11] S. K. Lau, S. K. Ho, "Open-circuit fault detection in distribution overhead power supply network," *Journal of International Council on Electrical Engineering*, 7:1, 269–275, 2017.
- [12] W. O'Brien, E. Udren, K. Garg, D. Haes, and B. Sridharan, "Catching Falling Conductors in Midair—Detecting and Tripping Broken Distribution Circuit Conductors at Protection Speeds," 42nd Annual Western Protective Relay Conference, Spokane, Washington, October 20–22, 2015.
- [13] Y. Yin, H. Bayat, N. Dunn M. Leyba, M. Webster, A. Marquez, K. Tran, and A. Torres, "High-speed Falling Conductor Protection for Electric Power Transmission Systems," 49th Annual Western Protective Relay Conference, Spokane, Washington, October 11–15, 2022.
- [14] S. E. Zocholl, "Three-Phase Circuit Analysis and the Mysterious k0 Factor," Proceedings of the 48th Annual Conference for Protective Relay Engineers, April 1995.
- [15] E. L. Harder, "Sequence Network Connections for Unbalanced Load and Fault Conditions," *The Electric Journal*, V. 34, December 1937, pp. 481–488.

## X. BIOGRAPHIES

**Kanchanrao Dase** received his bachelor of engineering degree in electrical engineering in 2009 from Sardar Patel College of Engineering, University of Mumbai, India. He received his master of science degree in electrical engineering from Michigan Technological University, Houghton, MI, in 2015. From 2009 to 2014, he was a manager at Reliance Infrastructure Limited with a substation engineering and commissioning profile. Currently, he is working with Schweitzer Engineering Laboratories, Inc. (SEL) as a lead power engineer. His research interests include power system protection, substation automation, and fault locating. He is an active IEEE member and has authored several technical papers relating to power system protection and automation. He currently holds five patents in power system protection.

**James Colwell** received his BA in Physics from University of Montana in 1995. He held the positions of President and principal designer for Green Energy Systems, Inc. from 2004 to 2012, where he worked in photovoltaic and thermal solar energy system design and installation. In 2016, James earned his MSEE from Montana Tech of the University of Montana and joined Schweitzer Engineering Laboratories, Inc as an associate power engineer. He currently holds the title of lead power engineer and works primarily on protective relay development in Pullman, Washington. His areas of interest include distributed energy resource protection, transmission, and distribution protection. James is an IEEE member and has authored and contributed to several technical papers relating to power system control.

**Shreenivas Pai** received his B.E. degree in Electrical Engineering from Atharva College of Engineering, University of Mumbai, India in 2016. He graduated with an MSE degree in Electrical Engineering from Arizona State University in 2019. He previously worked with Sterling & Wilson Pvt Ltd., an EPC in Mumbai, India from 2016 to 2017 as a trainee engineer in solar rooftop sales and engineering department. Since 2019, he has been working as a product engineer in R&D at Schweitzer Engineering Laboratories, Inc. His areas of interest include power system protection, distributed energy resources and control of power electronic converters for renewable energy applications.